

Short Wavelength Density and Low Frequency MHD Fluctuation Measurements in the STOR-M Tokamak

C. Xiao, S. J. Livingstone, A. K. Singh, D. Raju¹, G. St. Germaine, D. Liu, C. Boucher², A. Hirose
 Plasma Physics Laboratory, University of Saskatchewan, Saskatoon, Canada
 E-mail: chijin.xiao@usask.ca

Abstract. In the Saskatchewan Torus-Modified (STOR-M) tokamak, measurements of short wavelength density fluctuations during Ohmic discharges have been conducted using a small angle microwave scattering system. Long wavelength modes in the edge region have been measured with an array of Langmuir probes. The anticipated poloidal asymmetry of the Geodesic Acoustic Mode has been identified. Measurements using discrete Mirnov coils indicate that the Mirnov oscillations are suppressed during the H-mode like phase induced by compact torus injection. Furthermore, the MHD mode changes from $m = 4$ during the normal discharge phase to the $m = 1$ and $m = 2$ modes during the improved discharge phase.

1. Introduction

The effects of MHD activities on plasma confinement and the disruption-free operation of a tokamak reactor remain important topics in fusion research. In reversed magnetic shear configuration, ion energy confinement comparable to the neoclassical prediction has been achieved in the internal transport barrier (ITB), characterized by rapid plasma rotation associated with a nonuniform, strong radial electric field. However, electron energy confinement remains anomalous and it has been widely attributed to plasma turbulence and instabilities at various scale lengths. Of particular interest are short wavelength modes potentially caused by the ETG mode and density fluctuations in the regime of the electron collisionless skin depth $k_{\perp} \approx \omega_{pe} / c$ [1]. In the long wavelength regime, it has been predicted that zonal flows (ZFs) play an important role in regulating transport through saturation of the turbulence. The higher frequency branch of ZFs is due to non-vanishing divergence of the poloidal $\mathbf{E} \times \mathbf{B}$ rotation in the toroidal geometry and has been termed as geodesic acoustic mode (GAM) [2-4] with a characteristic oscillation frequency given by $\omega_{GAM} \approx c_s / R$, where c_s is the local ion sound speed and R is the major radius. It is noted that the pressure perturbation associated with the GAM mode is proportional to $\sin \theta$ where θ is the poloidal angle measured from the outer midplane [5].

It is recognized that MHD activities in a tokamak reactor must be managed to avoid major disruptions which could cause structural failure due to excessive induced image current. Identification of the MHD precursor and control of the MHD activities using feedback loops is important for a large tokamak. In a proposed scenario to fuel a tokamak reactor with a compact torus (CT) [6, 7], the MHD activities induced by merging of the CT and tokamak magnetic fields have to be studied. In previous tangential CT injection experiments on STOR-M, H-mode like discharges have been induced. While the $m = 2$ Mirnov oscillations are suppressed during the H-mode phase, the $m = 3$ Mirnov oscillations remain unchanged. Furthermore, the increase in both $m = 2$ and $m = 3$ Mirnov oscillations appeared to be the precursor for triggering the H-L back transition. More detailed studies of the CT injection on MHD activities are needed.

In this paper, we wish to report on the short wavelength density fluctuations measured by a 2 mm microwave scattering system, the long wavelength GAM and its poloidal

¹Institute for Plasma Research, Bhat, Gandhinagar, India

²INRS-EMT, Varennes, Canada

asymmetry measured at the STOR-M tokamak edge, and the global MHD activities measured by external Mirnov coils.

2. Experimental Setup

The experiments were conducted on the STOR-M tokamak [8]. STOR-M is an ohmically heated tokamak with a major radius of 46 cm and minor radius of 12 cm. It is equipped with a horizontal position feed-back control system. A combination of a horizontal rail limiter at $r = 12$ cm and a circular limiter at $r = 13$ cm near the mid-plane, both made of stainless steel, allows the plasma column to move horizontally ± 1 cm without being scraped off. During the experiments reported in this paper, the tokamak plasma parameters were monitored with various diagnostics. A 4 mm microwave interferometer was used to measure the electron density averaged along the central vertical chord. A monochromator aiming horizontally through the center of the chamber was used to monitor the H_α emission intensity. For a typical STOR-M discharge, the toroidal magnetic field (B_t) was 0.7 T, plasma current (I_p) 20 kA, and electron density in the range $(0.5 \sim 2) \times 10^{13}$ cm⁻³.

The University of Saskatchewan Compact Torus Injector (USCTI) forms and accelerates a compact torus (CT) to a velocity approximately 150 km/s [7]. The CT was injected tangentially into STOR-M during the current flat top phase from the outboard of the mid-plane at an angle of 27° with respect to the local major radius direction.

STOR-M is also equipped with a 2 mm homodyne microwave scattering system [9]. A Schottky-Barrier GaAs diode was used to detect the scattered signals. The STOR-M geometry restricts measurements of density fluctuations to the range $k \sim 5 - 10$ cm⁻¹.

Localized plasma density and floating potential fluctuations were measured using Langmuir probe arrays. To investigate the anticipated poloidal asymmetry of GAM fluctuations, four sets of Langmuir probe arrays were installed at the horizontal mid-plane ($\theta = 0^\circ$), top ($\theta = 90^\circ$), bottom ($\theta = 270^\circ$) and at $\theta = 315^\circ$, all at a fixed toroidal location. The probe sets can also be moved radially across the scrap-off layer (SOL) and the edge region. Each probe array has radially and poloidally separated pin pairs, allowing analyses of the wavenumber spectra of density/potential fluctuations using the two-probe method implemented by Beall *et al.* [10]. The signals are digitized using a simultaneous multichannel data acquisition system at a sampling speed of 1 microsecond per sample.

The global MHD fluctuations are monitored using $m = 2, 3$ Mirnov coils and 12 discrete Mirnov coils evenly distributed at a fixed toroidal location at poloidal angles $\theta = (i + 0.5) \times 30^\circ$ where $i = 0, 1, \dots, 11$. The outer mid-plane corresponds to $\theta = 0^\circ$. The coils are located outside the thin stainless steel bellows of the vacuum chamber.

3. Experimental results

3.1. Short wavelength density fluctuations

Figure 1(a) shows the spectral density function of the density fluctuations measured by the microwave scattering system. The power decreases steeply when k increases from 5 cm⁻¹ to 10 cm⁻¹. The measured spectral density function indicates that the spectrum should peak at $\bar{k} < 5$ cm⁻¹. In the STOR-M tokamak, the plasma β is small and the electron skin depth and ion Larmor radius are comparable. The estimated density fluctuation level in the plasma is $\bar{n}/n \approx 0.1$ at an average wave number of $\bar{k} \approx 7$ cm⁻¹. For the low β STOR-M plasma, the

estimated scaling parameters are $1/\bar{k}L_n \sim \rho_s/L_n \sim 0.015$, where L_n is the density scale length and ρ_s the ion Larmor radius with electron temperature. Scaling of the relative density fluctuation level with $1/\bar{k}L_n$ observed on STOR-M is consistent with the approximation from mixing length theory and experimental observations in other tokamaks [11].

The frequency and wavenumber have been extracted from the measured density fluctuation spectra based on statistical methods. Figure 1(b) shows the dispersion relation, the normalized frequency vs. the normalized wavenumber. Different symbols represent the results obtained with different STOR-M discharge conditions achieved by varying the toroidal field (20%), plasma current (80%), electron density (50%), and the resultant electron temperature (40%). The solid line is the lowest order dispersion relation expected from the drift mode. The observed frequency is too high and may suggest that electron dynamics is playing roles, including a long wavelength regime of the ETG mode with $k_{\perp} \approx \omega_{pe}/c$ [12]. The normalized frequency in short wavelength regime $k_{\perp}\rho_s > 1$ approaches a constant as expected of the skin size drift mode $\omega_r \approx \omega_{De}$, the electron magnetic drift frequency.

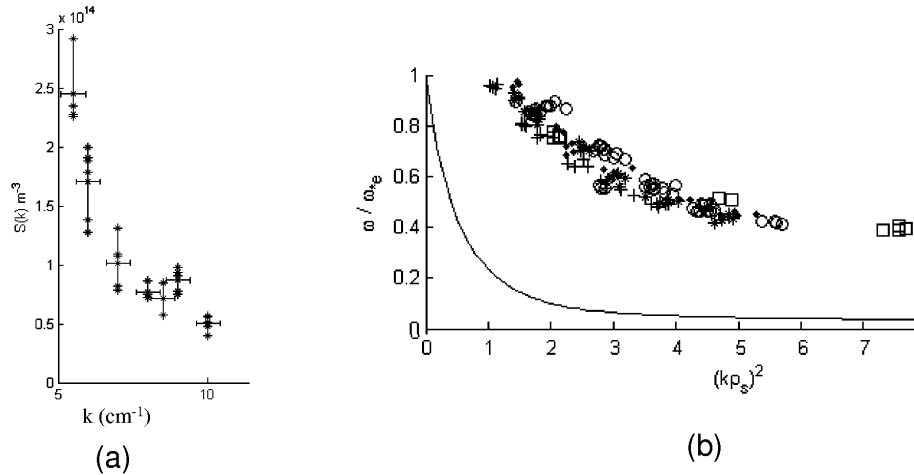


Fig. 1 (a) Spectral density function during a typical low plasma current discharge. Horizontal error bars are $\pm 0.4 \text{ cm}^{-1}$ and vertical bars represent the range of the data. (b) plot of the normalized average frequency vs. $(k\rho_s)^2$. The solid line represents the first order drift wave solution.

3.2. Geodesic Acoustic Mode

In the STOR-M SOL region, the frequency spectra of potential and density fluctuations measured by Langmuir probes exhibit a broadband turbulent power spectrum in the range of 5-100 kHz. The frequency spectrum in the edge region is similar to that in SOL except that a coherent peak at about 13 kHz emerges in the edge region as shown in Fig. 2. This peak is absent in the SOL region in spite of good bandwidth resolution. Using the temperature measured by Langmuir probes, the estimated frequency of the geodesic acoustic mode in the edge region of STOR-M is about 13 kHz, consistent with the observations.

GAM's are a branch of zonal flows and are characterized by $k_\theta = 0$ and $k_r \neq 0$. The measured dispersion relations of the potential fluctuations are plotted in Fig 3. It can be clearly seen within experimental uncertainties that the poloidal wavenumber vanishes while the radial wavenumber values are finite for the frequency range 13-15 kHz. This indicates that the observed peak at 13 kHz can be attributed to the GAM oscillations.

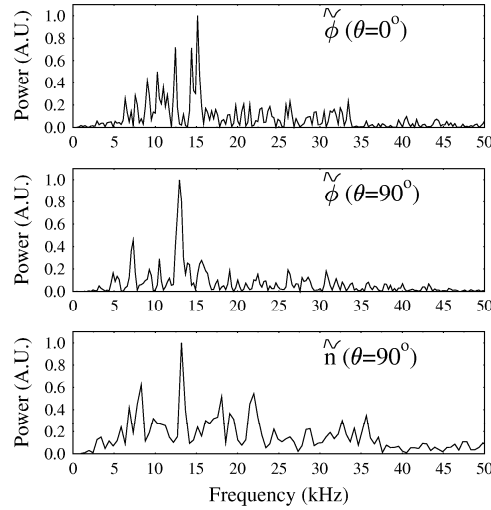


Fig. 2. Power spectrum of floating potential and density fluctuations. The peak at 13 kHz can be seen in all three signals.

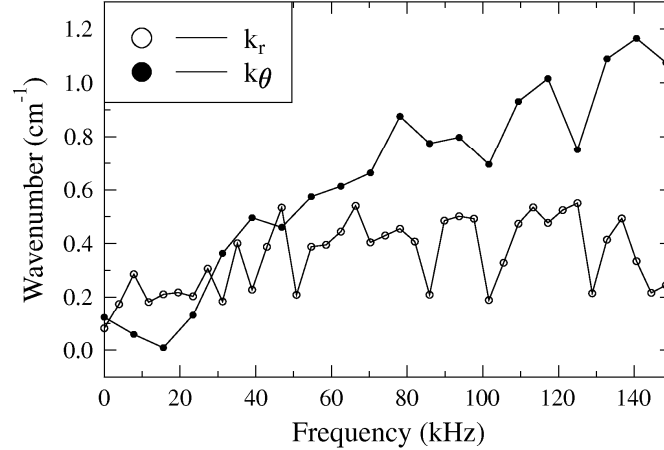


Fig. 3. The radial and poloidal wavenumber spectra of potential fluctuations.

It has been found theoretically that the amplitude of density fluctuations due to GAM obey a sinusoidal dependence on the poloidal angle. Figure 4 shows the power spectrum of density fluctuations at the poloidal angle $\theta = 0^\circ$. It is clearly seen that the peak at 13 kHz is absent from the density fluctuations. In contrast, both density and potential fluctuations at all other azimuthal angles have this peak (Fig. 3). We were not able to quantitatively verify a sinusoidal relationship in amplitude because of a steep temperature gradient and uncertainties in the probe positioning. However the results presented do suggest unambiguously that the measured peak at 13 kHz is consistent with the poloidal asymmetry predicted for GAM oscillations.

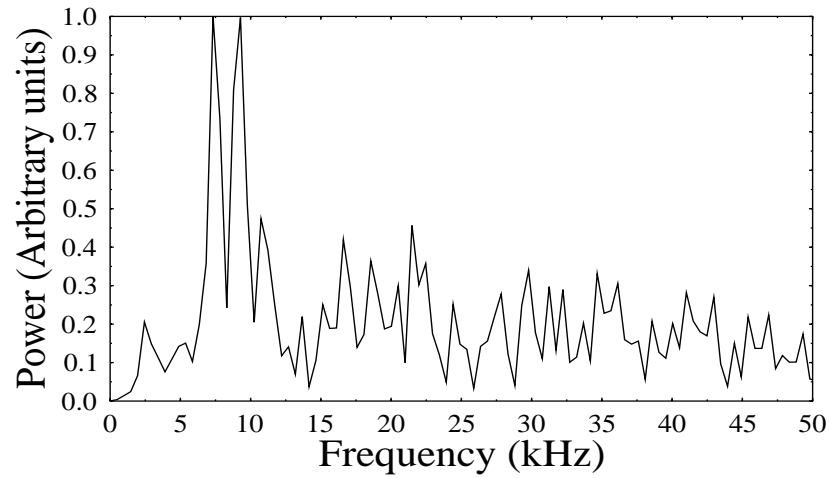


Fig. 4. The power spectrum of density fluctuations at $\theta=0^\circ$. The peak at 13 kHz is missing.

Figure 5 shows the time-frequency diagram of the potential fluctuations obtained with wavelet analysis. It clearly shows the dominant frequency at about 13 kHz as well as the intermittent streamer features.

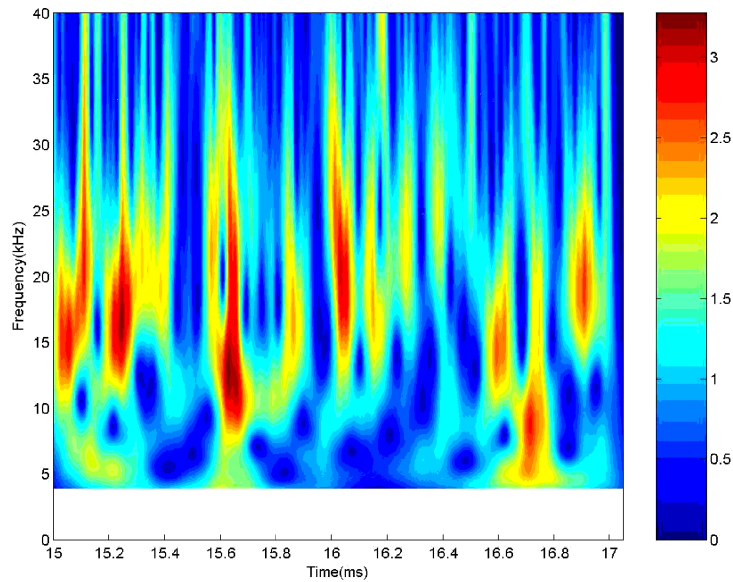


Fig. 5. Wavelet transform of potential fluctuations.

3.2. Magnetic fluctuations

In this section, we describe the features of the MHD oscillations observed on STOR-M particularly the effect of compact torus (CT) injection on the magnetic fluctuations. Figure 6 shows the plasma current in the top panel and the magnetic oscillations measured by one of the discrete magnetic pickup coils in the lower panel.

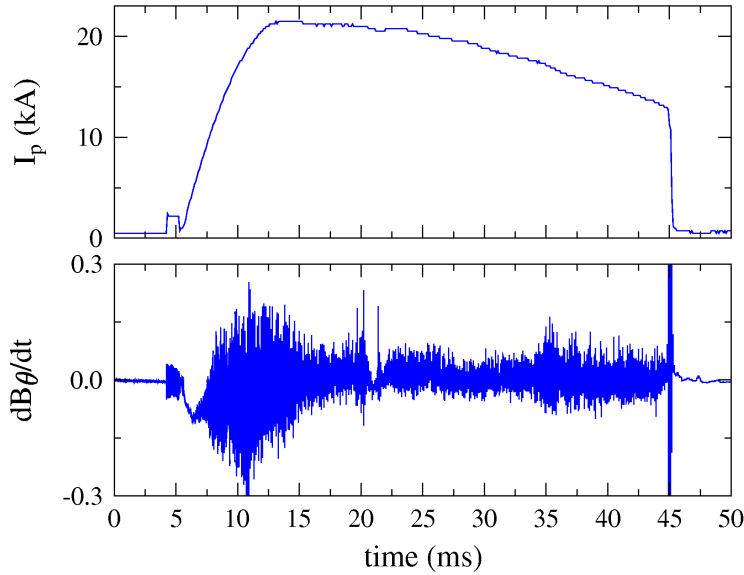


Fig. 6. The plasma current and a typical magnetic pickup coil signal. A compact torus is injected into the STOR-M discharge at $t=20.1$ ms.

In Fig. 7, we have plotted the temporal structure of these modes as a contour plot. Propagation of the MHD fluctuations can be seen in this figure. The ‘S’ shaped stripes are due to toroidal effects. A closer look at the signals reveals the presence of more than one mode at any given time. The conventional method to analyze these signals is based on Fourier methods. In this method, one determines the phases at the frequency of interest and then an attempt is made to find a best fit to the phases. It is assumed that each mode (m, n) has a distinct fixed frequency and the method fails in the presence of mode coupling. A typical mode coupling is indicated by two or more modes having the same frequency [13,14]. In the method utilized in this paper, correlation analysis is done in space rather than in time. The method itself is fairly new and has been described in detail [15]. The singular value decomposition (SVD) method is applied to a time-space matrix of multichannel Mirnov coil data. The singular values and principal axes contain information about the MHD mode. Mode structure can be seen as a polar plot of principal axes vs. probe positions.

On STOR-M, there is a set of 12 magnetic coils installed to detect fluctuations in the poloidal magnetic field. The data has been normalized to between -0.5 to 0.5 for the SVD analysis. Detailed analysis for discharge # 82960 has been carried out. In this shot a compact toroid was injected in the plasma at 20.1 ms marked by a noise spike shown in Fig. 6 (tokamak discharge starts at 5 ms with this time scale). CT injection induces H-mode like behaviors where the fluctuation amplitude drops right after the CT injection. Other signatures of an H-mode have also been observed in these shots, namely, reduction of H_{α} , and an increase in the line averaged density.

Three time instants have been chosen for the analysis. First we analyze the result at 17 ms in the discharge. This time instant is in the flat top region of the discharge and corresponds to the temporal mode structure in the top panel of Fig. 7. The lower left panel in this figure shows the amplitude vs. time of a pickup coil signal. The lower right plot shows spatial mode structure at a particular time, indicating an $m=4$ mode. The presence of higher mode numbers with the same frequency can be seen as a distortion in the mode structure. The poloidal asymmetry with breakage of the stripe, possibly related to twisted magnetic islands, in the high field side ($\theta = \pi$) is also apparent.

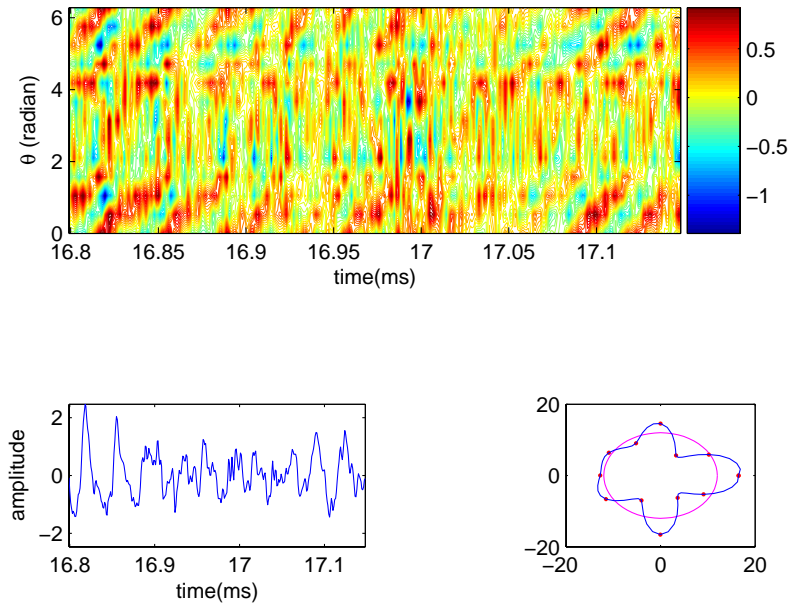


Fig.7. Temporal and spatial mode structure at $t= 16.8$ ms.

Figure 8 shows the temporal and spatial mode structure immediately after CT injection. Note the suppression in fluctuation amplitude after the CT injection. We can clearly see the loss in coherent propagation structure from the plot in the top panel. The spatial structure shows an $m = 1$ mode. After about 1 ms of this initial suppression phase, there is a relaxation type phenomenon after which the fluctuation level comes back to the normal level before CT injection. The analysis during this phase reveals the $m = 2$ mode structure and that the ‘S’ shaped stripe structure in propagation due to toroidal effects [14] are not seen during this time period.

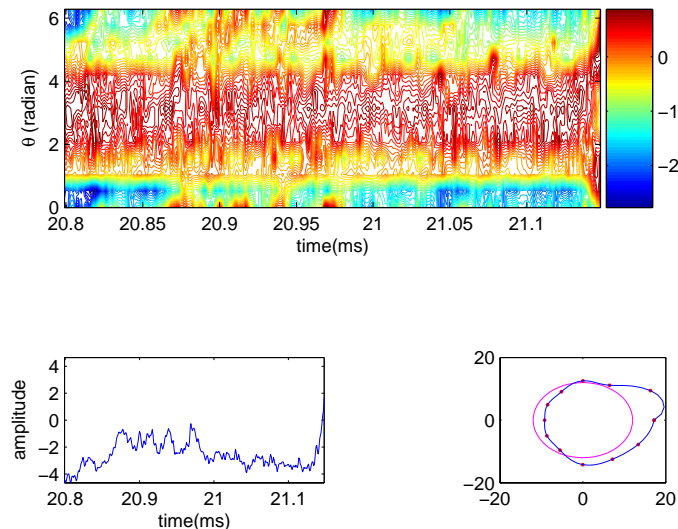


Fig. 8 Temporal and spatial mode structure at $t= 20.8$ ms, after CT injection at $t=20.1$ ms.

The mode structure at the time $t = 40$ ms is also determined. The structure is back to $m = 4$ as shown in Fig. 7. Thus, it can be summarized that in the flat top of the plasma current the most prominent mode is $m = 4$. During the fluctuation suppression phase induced by CT injection, the $m = 1$ and $m = 2$ modes are most prominent.

4. Conclusions

Short wavelength density fluctuations in the STOR-M tokamak have been measured by a 2 mm microwave scattering system. The measured relative density fluctuation level scales with $1/\bar{k}L_n$, as commonly found in other tokamaks. The spectral density function of the density fluctuations suggests that the drift type instabilities and skin size ETG mode may be the source of the density fluctuations. We have also reported on the poloidal structure of GAM in the STOR-M device based on the Langmuir probe measurement in a poloidal plane in the plasma edge region. The 13 kHz peak corresponding to GAM in our device is seen in all measured poloidal locations in potential signals. It is also seen in the density fluctuation signals at all poloidal locations except $\theta = 0^\circ$. This clearly demonstrates the dependence of GAM on the poloidal angle. We further verified the wavenumber spectra and showed the localization of the mode in the radial direction.

A set of 12 magnetic coils have been used to study the global MHD fluctuations in STOR-M in normal and H-mode like discharge phases. The H-mode induced by injection of a compact torus into the plasma is accompanied by reduction in Mirnov oscillation levels and a change in the spatial mode structures.

This work has been sponsored by the Canada Research Chair (CRC) program and the Natural Sciences and Engineering Research Council (NSERC) of Canada. Technical assistance provided by D. McColl is gratefully acknowledged.

References:

- [1] A. Hirose, Phys. Fluids B **3**, 1599 (1991); A. Hirose, and M. Elia, Phys. Scripta **65**, 257 (2002).
- [2] N. Winsor, J.L. Johnson, and J.M. Dawson, Phys. Fluids **11**, 2448 (1968).
- [3] K. Hallatschek, and D. Biskamp, Phys. Rev. Letts. **86**, 1223 (2001).
- [4] M. Ramisch, U Stroh, S. Neidner, and B. Scott, New J. Phys. **5**, 12 (2003).
- [5] A. Kramer-Flechen, *et al.*, Phys. Rev. Lett. **97**, 045006 (2006).
- [6] R. Raman, *et al.*, Phys. Rev. Letts. **86**, 1223 (2001);
- [7] S. Sen, C. Xiao, A. Hirose, and R.A. Cairns, Phys. Rev. Lett. **88**, 185001 (2002).
- [8] W. Zhang, C. Xiao, L. Zhang, and A. Hirose, Phys. of Plasmas **1**, 3646 (1994).
- [9] S. Livingstone, "Experimental Study of Density Fluctuations in the STOR-M Tokamak by Small-Angle Microwave Scattering", M.Sc Thesis, University of Saskatchewan, 2005
- [10] J.M. Beall, Y.C. Kim, and E.J. Powers, J. Appl. Phys. **53**, 3933 (1982).
- [11] C.M. Surko, and R.E. Slusher, Science **221**, N4613, p817 (1983).
- [12] N. Joiner, and A. Hirose, 21st IAEA Fusion Energy Conference, Chengdu, paper no. TH/P2-7.
- [13] O. Kluber, H. Zohm, and H. Bruhms *et al.*, Nucl. Fusion **31**, 907 (1991).
- [14] C. Nordone, Plasma Phys. Control. Fusion **34**, 1447 (1992).
- [15] T.R. Harley, D.A. Buchenauer, J.W. Coonrod, and K.M. McGuire, Nucl. Fusion **29**, 771 (1989).